Experimental realization of a low-noise heralded single-photon source

G. Brida,[1] I. P. Degiovanni,[1*] M. Genovese,[1] A. Migdall,[2] F. Piacentini,[1] S. V. Polyakov,[2] I. Ruo Berchera[1]

[1] *I.N.RI.M., Strada delle Cacce 91, 10135 Torino, Italia*
[2] *Joint Quantum Institute and National Institute of Standards and Technology, 100 Bureau Dr, Stop 8441, Gaithersburg, MD, 20899 USA*

[*] *i.degiovanni@inrim.it*

Abstract: We present a heralded single-photon source with a much lower level of unwanted background photons in the output channel by using the herald photon to control a shutter in the heralded channel. The shutter is implemented using a simple field programable gate array controlled optical switch.

OCIS codes: (270.0270) Quantum optics; (270.5585) Quantum information and processing.

References and links

1. http://www.quantumcandela.net.
2. G. Brida, M.Genovese, and M. Gramegna, "Twin-Photon techniques for photo-detector calibration," Laser Phys. Lett. **3**, 115-123 (2006).
3. S. V. Polyakov and A. L. Migdall, "Quantum radiometry," J. Mod. Opt. **56**(9), 10451052 (2009) *and refs. therein.*
4. R. Thew and N. Gisin, "Quantum communication," Nature Photon. **1**, 165171 (2007) *and refs. therein.*
5. J. L. O'Brien, A. Furusawa, and J. Vickovic, "Photonic quantum technologies," Nature Photon. **3**, 687-695 (2009) *and refs. therein.*
6. M. Genovese, "Research on hidden variable theories: A review of recent progresses," Phys. Rep. **413**, 319-396 (2005) *and refs. therein.*
7. G. Brida, I.P. Degiovanni, M. Genovese, V. Schettini, S. Polyakov, and A. Migdall, "Experimental test of non-classicality for a single particle," Opt. Express, **16**, 11750-11758 (2008).
8. G. Brida, I. P. Degiovanni, M. Genovese, F. Piacentini, V. Schettini, N. Gisin, S. V. Polyakov, and A. Migdall, "Improved implementation of the AlickiVan Ryn nonclassicality test for a single particle using Si detectors," Phys. Rev. A **79**, 044102 (2009).
9. P. Grangier, G. Roger, and A. Aspect, "Experimental evidence for a photon anticorrelation effect on a beam splitter: a new light on single-photon interferences," Europhys. Lett. **1**, 173-179 (1986).
10. D. N. Klyshko, "Utilization of vacuum fluctuations as an optical brightness standard," Kvant. Elektron. (Moscow) **4**, 10561062 (1977) [Sov. J. Quantum Electron. **7**, 591595 (1977)].
11. C. K. Hong and L. Mandel, "Experimental realization of a localized one-photon state," Phys. Rev. Lett. **56**, 58-60 (1986).
12. A. B. U'Ren, C. Silberhorn, K. Banaszek, and I.A. Walmsley, "Efficient conditional preparation of high-fidelity single photon states for fiber-optic quantum networks," Phys. Rev. Lett. **93**, 093601 (2004).
13. S. Castelletto, I. P. Degiovanni, V. Schettini, and A. Migdall, "Spatial and spectral mode selection of heralded single photons from pulsed parametric down-conversion," Opt. Express **13**, 6709-6722 (2005).
14. S. Fasel, O. Alibart, S. Tanzilli, P. Baldi, A. Beveratos, N. Gisin, and H. Zbinden, "High-quality asynchronous heralded single-photon source at telecom wavelength," New J. Phys. **6**, 163 (2004).
15. A. B. URen, C. Silberhorn, J. L. Ball, K . Banaszek, and I. A. Walmsley, "Characterization of the nonclassical nature of conditionally prepared single photons," Phys. Rev. A **72**, 021802(R) (2005).
16. G. P. Agrawal, *Nonlinear Fiber Optics*, 2nd ed. (Academic Press, New York, 1995).
17. J. Fan and A. Migdall, "A broadband high spectral brightness fiber-based two-photon source," Opt. Express **15**, 2915-2920 (2007).
18. J. Fan, M. D. Eisaman, and A. Migdall, "Bright phase-stable broadband fiber-based source of polarization-entangled photon pairs," Phys. Rev. A **76**, 2043836 (2007).

#133346 - $15.00 USD Received 13 Aug 2010; revised 24 Sep 2010; accepted 22 Oct 2010; published 13 Jan 2011

19. J. Fan, M. D. Eisaman, and A. Migdall, "Quantum state tomography of a fiber-based source of polarization-entangled photon pairs," Opt. Express **15**, 18339-18344 (2007).
20. J. Fulconis, O. Alibart, J. L. OBrien, W. J. Wadsworth, and J. G. Rarity, "Nonclassical Interference and Entanglement Generation Using a Photonic Crystal Fiber Pair Photon Source," Phys. Rev. Lett. **99**, 120501 (2007).
21. C. Kurtsiefer, M. Oberparleiter, and H. Weinfurter, "High-efficiency entangled photon pair collection in type-II parametric fluorescence," Phys. Rev. A **64**, 023802 (2001).
22. F. A. Bovino, P. Varisco, M. A. Colla, G. Castagnoli, G. Di Giuseppe, and A. V. Sergienko, "Effective Fiber-coupling of Entangled Photons for Quantum Communication," Opt. Commun. **227**, 343-348 (2003).
23. S. Castelletto, I.P. Degiovanni, A. Migdall, and M. Ware, "On the measurement of two-photon single mode coupling efficiency in PDC photon sources," New J. Phys. **6**, 87 (2004).
24. A. Fedrizzi, T. Herbst, A. Poppe, T. Jennewein, and A. Zeilinger, "A wavelength-tunable fiber-coupled source of narrowband entangled photons," Opt. Express **15**, 15377-15386 (2007).
25. T. Horikiri, Y. Takeno, A. Yabushita, and T. Kobayashi, "Photon-number-resolved heralded-photon source for improved quantum key distribution," Phys. Rev. A. **76**, 012306 (2007).
26. A. Migdall, "Correlated-Photon Metrology Without Absolute Standards," Phys. Today **52**, 41-46 (1999).
27. A. L. Migdall, D. Branning, and S. Castelletto, "Tailoring Single and Multiphoton Probabilities of a Single Photon On-Demand Source," Phys. Rev. A **66**, 053805(2002).
28. E. Jeffrey, N. A. Peters, and P. G. Kwiat, "Towards a periodic deterministic source of arbitrary single-photon states," New J. Phys. **6**, 100 (2004)
29. S. Takeuchi, R. Okamoto, and K. Sasaki, "High-yield single-photon source using gated spontaneous parametric downconversion," Appl. Opt. **43**, 57085711 (2004)
30. M. Oxborrow and A. C. Sinclair, "Single-photon sources," Contemp. Phys. **46**, 173-206 (2005).
31. S. Scheel, "Single-photon sources- an introduction," J. Mod. Opt. **56**, 141-160 (2009).
32. P. Grangier, G. Roger, and A. Aspect, "Experimental evidence for a photon anticorrelation effect on a beam splitter: a new light on single-photon interferences," Europhys. Lett. **11**, 173-179 (1986).
33. G. Brida, M. Genovese, M. Gramegna, and E. Predazzi, "A conclusive experiment to throw more light on light," Phys. Lett. A **328**, 313-318 (2004).
34. J. Vuckovic, D. Fattal, C. Santori, G. S. Solomon, and Y. Yamamoto, "Enhanced single-photon emission from a quantum dot in a micropost microcavity," Appl. Phys. Lett. **82**, 3596 (2003).
35. A. Bennett, D. Unitt, P. Atkinson, D. Ritchie, and A. Shields, Opt. Express **13**, 50-55 (2005).
36. M. Keller, B. Lange, K. Hayasaka, W. Lange, andH. Walther, "Continuous generation of single photons with controlled waveform in an ion-trap cavity system," Nature **431**, 1075-1078 (2004).
37. http://www.eospace.com/Switches.htm
38. Certain commercial equipment, instruments or materials are identified in this paper to foster understanding. Such identification does not imply recommendation or endorsement by the National Institute of Standards and Technology, nor does it imply that the materials or equipment are necessarily the best available for the purpose.
39. All the uncertainties and the error bars correspond to the coverage factor $k = 1$ except for the 95% confidence bands of Fig. 3.
40. R. H. Hadfield, "Single-photon detectors for optical quantum information," Nature Photon. **3**, 696-705 (2009) *and references therein.*

While ideal single-photon sources are desired for many applications from metrology [1–3], to quantum information [4, 5], to analytical methods, to foundations of quantum mechanics [6–8], the best that can be achieved are sources that offer some approximation to such a source.

One commonly used approximation is the heralded-photon source which relies on photons produced in pairs, where one of the photons is used to herald the existence of the other photon. While a useful device, this type of source suffers from two particular deficiencies, and these deficiencies have afflicted pair sources from the earliest ones based on atomic cascade [9], to parametric down conversion (PDC) [10–15] in crystals, to four-wave mixing in fibers [16–20]. One deficiency is that the production is probabilistic and the other is that the probability of extraction of each of the photons of a pair is independent and less than unity. An important point about this first deficiency is that a probabilistic source must be operated at generation rates much below one photon or pair per pulse to avoid creation of multi-photon states and loss after creation cannot be compensated by increasing the generation rate. The second deficiency results in many heralding counts that yield no output photon and conversely many photons are emitted from the output channel without a heralding count. Both of these failure modes can present problems for particular applications and are worthy of efforts to reduce their likeli-

#133346 - $15.00 USD Received 13 Aug 2010; revised 24 Sep 2010; accepted 22 Oct 2010; published 13 Jan 2011

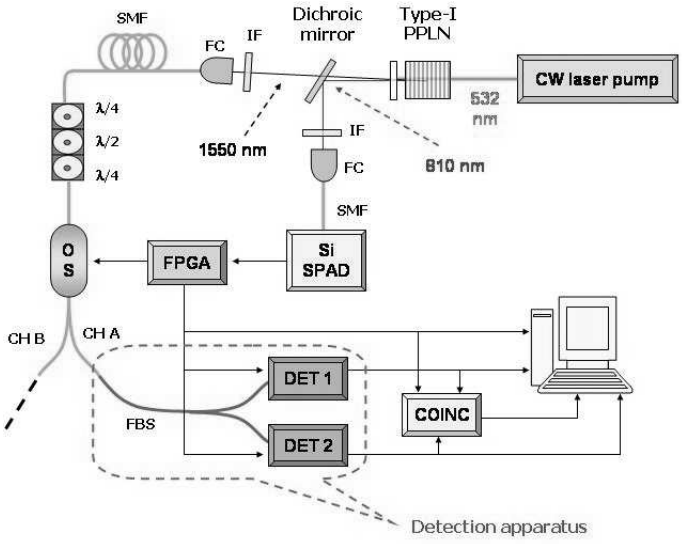

Fig. 1. Experiment arrangement. Channel A is the low-noise HSPS output. Channel B is sent to a beam dump.

hood. Both deficiencies can be reduced by improving the photon extraction efficiency and there are efforts in that direction [13, 21–24]. To further reduce the emission of unheralded photons beyond improving the extraction efficiency, several strategies have been proposed and implemented. For example, using a photon-number-resolving detector on the heralding arm highlights the presence of multi-photon emission from the heralded arm [25]. Another approach exploits the use of an optical shutter, where the optical output path is blocked unless a photon is known to be incident. This simple idea has been discussed for some time [10, 26], but source development efforts have been focused more on the production of single-photon sources "on-demand" [27–29], rather than on the suppression of unheralded photons. Instead, fast InGaAs-based gated avalanche photo diode detectors were used to avoid the consequences of photon noise in a heralded channel, see for example [14]. However, with the advent of single-photon technology and applications, the need for a *low-noise* heralded single-photon source has become more pressing. Particularly, detectors with high temporal jitter or slow temporal response (e.g., transition edge superconducting microbolometers that are superior to InGaAs detectors in their detection efficiency, and free of dark counts) suffer from background noise of conventional single photon sources. This is because the low time resolution does not allow for tight time discrimination between the desired heralded photons and unwanted background photons when a history-dependent process of photon interactions is studied or history-dependent detection is used. To compensate for this, data rates must often be reduced to very low levels, while if low-noise sources were available, data rates could be increased significantly. Reducing the noise of a heralded photon source would also improve single-photon applications such as radiometry, where knowing the number of emitted photons is key to the measurements. Noisy photon sources are also problematic for quantum information applications where additional unwanted photons make the already difficult task of processing a fragile quantum state that much more difficult.

We present here a heralded-photon source based on PDC with an optical shutter that opens for a short period of time around the expected emission time of a heralded photon. Because this scheme greatly reduces the emission of unheralded photons, we refer to this type of source as

#133346 - $15.00 USD Received 13 Aug 2010; revised 24 Sep 2010; accepted 22 Oct 2010; published 13 Jan 2011

a low-noise heralded-single-photon-source (HSPS). Despite the fact that significant further improvements in single-photon performance could be obtained, the current version of our source is already at the level of the best solid-state based single-photon sources [30, 31].

In our experimental setup (Fig. 1) a continuous wave (cw) laser ($\lambda = 532$ nm) pumps a $5 \times 1 \times 5$ mm periodically poled Lithium Niobate (PPLN) crystal, producing non-degenerate parametric down conversion signal and idler photons with wavelengths of $\lambda_s = 1550$ nm and $\lambda_i = 810$ nm, respectively.

The idler photon is sent to an interference filter (IF) with a full width half maximum (FWHM) of 10 nm, then fiber-coupled to a silicon single-photon avalanche detector (Si-SPAD). The signal photon is sent to a 30 nm FWHM filter (IF) and coupled to a 20 m long single-mode optical fiber connected to the optical switch (OS) controlled by a field programmable gate array (FPGA). We used an EO-space Ultra-High-Speed 2x2, polarization-dependent OS [37,38]. The switch technology is based on LiNbO3 Mach-Zehnder interferometer. Note that for best results in rejecting the unheralded photons, IFs with rectangular transmittance profiles that are exact conjugates with respect to pump wavelength should be used in addition to temporal filtering, however the effect of such filters would be quite insignificant (order of 3 at best) compared with extinction ratio of the OS (a factor of 100 or more). The OS channel A, chosen as our low-noise HSPS output channel, is connected to a 50%-50% fiber beam splitter (FBS) whose outputs are sent to two infrared InGaAs SPADs (DET_1 and DET_2), triggered by the same FPGA signal that triggers the optical switch. The InGaAs SPAD detection window was kept at a fixed 100 ns for all measurements for simplicity and easier comparison of those measurements. The outputs of the two InGaAs SPADs are sent to coincidence electronics with time-bin resolution of 2.5 ps and finally recorded by the computer. The FPGA triggers a pulse generator that opens the OS channel A for a time interval $\Delta t_{\mathrm{switch}}$ of only a few nanoseconds encompassing the passage of an 810 nm photon, and then switches to channel B for a chosen "shuttered" time t_{dead} before the system is ready to be retriggered by a Si-SPAD count. To reject InGaAs SPAD afterpulses, we set $t_{\mathrm{dead}} = 20\ \mu$s. We note that the minimum time increment achievable by our FPGA is 6 ns, thus, we are far from the performance limits of this technology. We made measurements with four different switch pulse durations $\Delta t_{\mathrm{switch}}$ (60 ns, 30 ns, 15 ns, and 5 ns).

Looking at the histogram of the detection window of DET_1 (Fig. 2(a)) we can distinguish three different "regions" corresponding to:

- $N^{(\mathrm{True})}$ = true heralded photon counts;
- $N^{(\mathrm{Bkg})}$ = counts due to background and stray light passing through the optical switch;
- $N^{(\mathrm{Dark})}$ = dark counts of the IR detector.

We define the true heralded photon detection probability (as seen by DET_1 and DET_2) for each trigger count as

$$P_i^{(\mathrm{True})} = \frac{N_i^{(\mathrm{True})}}{N_i^{(\mathrm{Trig})}} \qquad i = 1,2 \tag{1}$$

($P_i^{(\mathrm{Bkg})}$ and $P_i^{(\mathrm{Dark})}$ are analogously defined), where $N_i^{(\mathrm{Trig})}$ is the total number of trigger counts accepted by the i-th detector. Note that we have made the assumption that all events represented by Ps are mutually exclusive and independent of each other. This is a reasonable assumption in the situation where their values are small.
The overall detection probability of detector i is

$$P_i^{(\mathrm{Tot})} = P_i^{(\mathrm{True})} + P_i^{(\mathrm{Bkg})} + P_i^{(\mathrm{Dark})}. \tag{2}$$

#133346 - $15.00 USD Received 13 Aug 2010; revised 24 Sep 2010; accepted 22 Oct 2010; published 13 Jan 2011

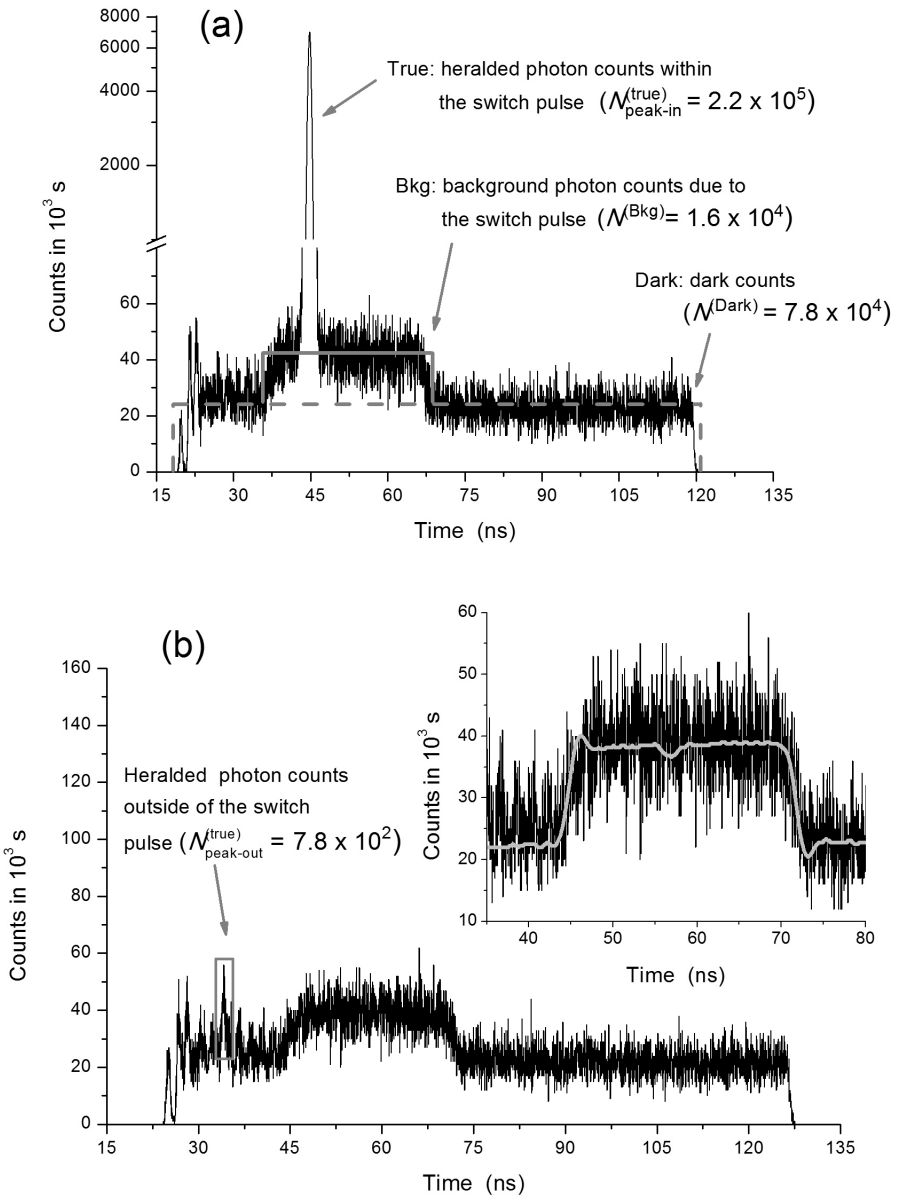

Fig. 2. Histograms of DET_1 100 ns detection window ($\Delta t_{\text{switch}} = 30$ ns, with 25 ps time bins). (a) The peak is inside the switch pulse region; true, background, and dark count contributions are clearly seen. (b) The heralded photon peak is outside of the OS active region thus it is highly suppressed. The inset shows a closeup of a switch-on region, with the solid line showing the shape of the electrical pulse driving the OS. The estimated integrals of true, background, and dark counts (measured in 1000 s corresponding to $N^{(\text{Trig})} = 3.52 \times 10^7$) are shown in the feature labels and defined in the text.

#133346 - $15.00 USD Received 13 Aug 2010; revised 24 Sep 2010; accepted 22 Oct 2010; published 13 Jan 2011

To evaluate these three probabilities, we look at the histogramed outputs of DET_1 and DET_2 in two different configurations: *peak-in* (Fig. 2(a)), with the heralded photons arriving during the OS open time, and *peak-out* (Fig. 2(b)), where the switching pulse is delayed with respect to the arrival of the heralded photons so that they do not arrive during the switch open time (i.e. during the pulse duration Δt_{switch}). To do so, the average photon number per detection bin is calculated for the intervals in Fig. 2 that are clearly attributed to the physical processes: dark count rate per bin is estimated in an interval from $\approx$ 75ns to $\approx$ 115ns; background count rate per bin is estimated in an interval from $\approx$ 50ns to $\approx$ 70ns, etc. Then, this average rate is multiplied by the number of bins where the effect is present (i.e. the dark counts are present during the entire 100 ns when the APD is active, and the background is present only when the OS is turned on). We can also directly measure OSs extinction ratio by comparing the area of the main correlation peak when it is fully transmitted by the OS (as in Fig. 2(a)) to that when it is rejected by the OS (as in Fig. 2 (b)).

We can then calculate the ratio of unwanted to total photons in our distribution channel. We call this parameter *Output Noise Factor* (*ONF*), defined as:

$$ONF = \frac{P_1^{(\text{Bkg})} + P_2^{(\text{Bkg})}}{P_1^{(\text{True})} + P_1^{(\text{Bkg})} + P_2^{(\text{True})} + P_2^{(\text{Bkg})}}. \tag{3}$$

The other figure of merit we consider for our HSPS is α (analogous to the second order correlation function $g^{(2)}(0)$ [32, 33]):

$$\alpha = \frac{P_{12}^{(\text{True+Bkg;True+Bkg})}}{P_1^{(\text{True+Bkg})} \cdot P_2^{(\text{True+Bkg})}}, \tag{4}$$

where $P_{12}^{(\text{True+Bkg;True+Bkg})}$ is the probability of a coincidence photon count between DET_1 and DET_2 (dark counts subtracted). Assuming $P_{12}^{(\text{True;True})} = 0$ (note that the probability of more than one photon within a 1 ns time interval, which is a generous estimate of the detector jitter time, is less than 10^{-9}), and $P_i^{(\text{Bkg})}$ and $P_i^{(\text{Dark})}$ are independent, we obtain:

$$P_{12}^{(\text{True+Bkg;True+Bkg})} = P_{12}^{(\text{Tot;Tot})} - P_{12}^{(\text{Dark;tot})} - P_{12}^{(\text{Tot;Dark})} + P_{12}^{(\text{Dark;Dark})}. \tag{5}$$

All the terms in Eq.(5) can be extracted from measurements made by blocking the light to each detector in turn.

Our results, summarized in Fig. 3(a,b), show the *ONF* decreasing linearly with the duration of Δt_{switch}, a direct consequence of the reduction in background photons as the OS on-time is narrowed. The values range from a maximum of 11.5% for $\Delta t_{\text{switch}} = 60$ ns to a minimum of 1.45% for $\Delta t_{\text{switch}} = 5$ ns, clearly showing the noise reduction in our source's output channel.

As expected, the parameter α shows the same behavior as the *ONF*, decreasing linearly with the switching time Δt_{switch}: it ranges from 0.253 ($\Delta t_{\text{switch}} = 60$ ns) to the remarkable value 0.0136 ($\Delta t_{\text{switch}} = 5$ ns), highlighting the advantage of our shuttered single-photon source. We note that our best measured α value ($\alpha = 0.0136$) is comparable or better than the best values obtained for single-photon emitters; for example, a quantum dot in micropillar with $\alpha = 0.02$ [34, 35] or $^{40}Ca^{+}$ in ion-trap cavity with $\alpha = 0.015$ [36]. Fig. 3(a) shows a linear fit to the data, where for the ideal case of $\Delta t_{\text{switch}} = 0$, we would obtain $\alpha = -0.003 \pm 0.025$, which is clearly compatible with 0, indicating that there are no other effects limiting the device performance at this level of uncertainty. In addition, we compare our low-noise source with the similar conventional PDC source where the noise in heralded channel was mitigated by postselection [14]. Such comparison yields similar performance in terms of α parameter for the equivalent

#133346 - $15.00 USD Received 13 Aug 2010; revised 24 Sep 2010; accepted 22 Oct 2010; published 13 Jan 2011

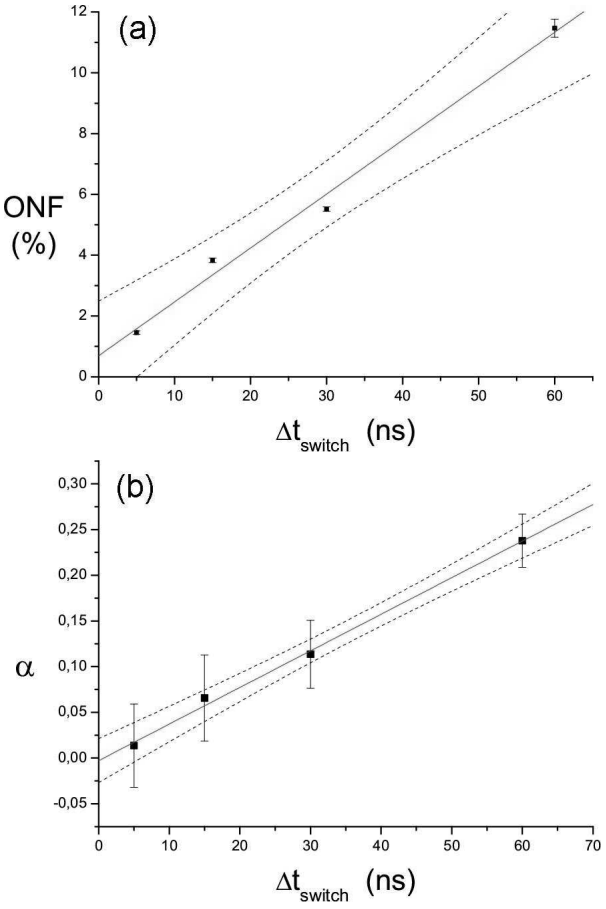

Fig. 3. (a) *ONF* and (b) α ($\simeq g^{(2)}(0)$) parameters versus the switching time Δt_{switch}. The linear fits (line) of the data (points) are shown along with 95% confidence bands (dashed curves).

heralding rates. However, independent of such comparison, we stress that uncorrelated photons are always present in a conventional source and their impact cannot be reduced by fast gating in history-dependent applications. For the ONF data in Fig. 3(a) we obtain $ONF = 0.70 \pm 1.8$, also consistent with zero. The uncertainties on the α data are larger than those obtained for the *ONF*, mainly because the double coincidence events needed to evaluate $P_{12}^{(\text{True+Bkg;True+Bkg})}$ are relatively rare (as can be seen in table 1), further highlighting the extremely low noise of our HSPS.

The main performance limitation, i.e. the lower bound for α that we achieved, is due to the slow rise/fall time of our pulse generator (≈ 2.5 ns, as seen in the inset plot of Fig. 2(b)) and the jitter of the Si-SPAD in the heralding arm (≈ 500 ps). Each of these limits the number of non heralded photons that can be rejected. The first by providing a minimum width of the switch open time and the second by adding uncertainty to the time between the opening of the switch (driven by the heralding events) and the presence of the heralded photon. This jitter is directly contributes to the width of the true coincidences peak (True) and clearly, Δt_{switch} must be kept larger than the full width of the peak itself (currently ≈ 3 ns). These are technical rather

#133346 - $15.00 USD Received 13 Aug 2010; revised 24 Sep 2010; accepted 22 Oct 2010; published 13 Jan 2011

Table 1. Data used to calculate α parameter for the switch-on duration of $\Delta t_{\text{switch}} = 5$ ns: every value is the average of 10 acquisitions of 100 s each, with a trigger count rates of 3.48×10^4 counts/s.

Configuration	P_2 $(\times 10^{-3})$	P_1 $(\times 10^{-3})$	P_{12} $(\times 10^{-5})$
Tot ; Tot	6.22 ± 0.01	7.90 ± 0.02	2.24 ± 0.09
Tot ; Dark	6.16 ± 0.02	2.27 ± 0.01	1.41 ± 0.09
Dark ; Tot	1.34 ± 0.01	7.83 ± 0.02	1.09 ± 0.03
Dark ; Dark	1.34 ± 0.01	2.27 ± 0.01	0.29 ± 0.03

than fundamental issues that can be overcome by using lower jitter commercially available Si-SPADs along with faster pulse generators leading to a possible $\Delta t_{\text{switch}} \leq 1$ ns. From the linear trends in Fig. 3(a,b) we would expect the values of ONF to be within 1 % of zero and α to be within 0.02 of zero at the 1 ns width that we believe is achievable.

To investigate the extinction performance of our OS, we compare the heralded photon peak within the switch-on time as in Fig. 2(a) with the corresponding residual peak of the heralded photon when it is out of the switch pulse duration as in Fig. 2(b), defining the extinction ratio between $P^{(\text{True})}$ in the peak-out and peak-in configurations:

$$r = \frac{P^{(\text{True})}_{\text{peak-out}}}{P^{(\text{True})}_{\text{peak-in}}}. \tag{6}$$

with a measured value of $r = 3.5 \times 10^{-3}$. To see more clearly what this means in terms of rejecting uncorrelated photons, we notice that for each Δt_{switch} value, the rate of incident noise photons per second, i.e. before the OS, can be obtained as:

$$F^{(\text{Bkg})} = \frac{P_1^{(\text{Bkg})} + P_2^{(\text{Bkg})}}{\Delta t_{\text{switch}}} \cdot \frac{1}{\eta}, \tag{7}$$

while after the optical switch the rate is:

$$f^{(\text{Bkg})} = F^{(\text{Bkg})} \cdot r \tag{8}$$

By substituting the appropriate numbers reported in Fig. 2, we obtain $F^{(\text{Bkg})} \simeq 3.5 \times 10^5$ photons/s without the switch and, $f^{(\text{Bkg})} \simeq 1.2 \times 10^3$ photons/s with the switch. In our implementation the emitted rate of true heralded photons is 4.5×10^3 photons/s, and is limited by the long shuttered time $t_{\text{dead}} = 20\mu$s that we imposed on the source by FPGA, in order to reduce afterpulsing in the detection apparatus. Without this artificial constraint, our source can reach the rate of 1.5×10^4 photons/s simply by setting $t_{\text{dead}} = 0$. Therefore, without the OS the heralded photons would be dispersed in the "noise" of background photoelectronic detections that contains 20x more photons than the heralded signal, while after the optical switch the background is reduced to less than 0.1x of the true heralded photon rate, eliminating the need for postselection. The calibration of our detection apparatus, composed of the fiber beam splitter and the two InGaAs SPADs, is made using a power-stabilized 1550 nm laser beam attenuated to the photon counting regime, giving an overall detection efficiency $\eta = (8.1 \pm 0.2)\%$ [39]. This calibration allows us to evaluate the coupling efficiency γ of our single-photon source, defined as:

$$\gamma = \frac{P_1^{(\text{True})} + P_2^{(\text{True})}}{\eta}. \tag{9}$$

#133346 - $15.00 USD Received 13 Aug 2010; revised 24 Sep 2010; accepted 22 Oct 2010; published 13 Jan 2011

The average of the coupling efficiencies obtained for each OS configuration is $\gamma = (14 \pm 1)\%$, and the singles measurements are independent of Δt_{switch}. We emphasize that better engineering, particularly, mitigating optical losses, and using collinear parametric down-conversion with optimized beam waists could increase γ significantly [24], while maintaining the low background of our single-photon source scheme.

In conclusion, we have presented an experimental implementation of a low-noise heralded single-photon source. The results obtained in terms of the single-photon parameters α and *ONF* are already comparable to the best solid-state based single-photon sources [30, 31]. As implemented, α and *ONF* are limited by the rise/fall time of the pulse generator controlling the optical switch and the jitter of the heralding detector, resulting in a minimum switch window of a few nanoseconds.

In addition, further improvements in α and *ONF* are expected with readily available components such as a detector with less than 100 ps jitter and an optical switch and associated drivers with sub-ns switching times, although care would have to be taken to assure good uniformity of switch transmission during such short pulses. We note that the inherent switching time of the optical switch used was 18 GHz.

We also note that, with respect to the other single-photon sources such as for example quantum dots, color centers in nanodiamond, etc. [30, 31], the low-noise heralded-single-photon source has the advantage of the wide wavelength tunability typical of PDC-based sources. Furthermore, because this source operates at telecom wavelengths, it can exploit commercially available telecom components, e.g., wavelength division multiplexing and/or narrow spectral selection by means of Bragg fiber filters.

The background photon rejection and the possibility of controlling and tuning the value of t_{dead} is particularly advantageous when dealing with slow response systems or slow detectors, such as for example, detectors with high temporal jitter or slow temporal response like transition edge superconducting microbolometers [40], where the slow response does not allow for temporal discrimination of unwanted events, allowing much higher detection rates, compared to conventional HSPSs.

Finally, the whole system can be integrated, or at least pigtailed, as the source can be realized with a PPLN waveguide, the same technology used for the fast OS.

Acknolwedgments

This work has been partially supported by PRIN 2007FYETBY (CCQOTS).

#133346 - $15.00 USD Received 13 Aug 2010; revised 24 Sep 2010; accepted 22 Oct 2010; published 13 Jan 2011